September 2001 • NREL/CP-500-30565

Conference Paper

Four-Point Bending Strength Testing of Pultruded Fiberglass Wind Turbine Blade Sections

Walter D. Musial, Ben Bourne, Scott D. Hughes
National Renewable Energy Laboratory

Michael D. Zuteck
MDZ Consulting

Presented at AWEA's WINDPOWER 2001 Conference
Washington, D.C.
June 4 – June 7, 2001

National Renewable Energy Laboratory

1617 Cole Boulevard
Golden, Colorado 80401-3393

NREL is a U.S. Department of Energy Laboratory
Operated by Midwest Research Institute • Battelle • Bechtel

Contract No. DE-AC36-99-GO10337

FOUR-POINT BENDING STRENGTH TESTING OF PULTRUDED FIBERGLASS WIND TURBINE BLADE SECTIONS

Walter D. Musial
Ben Bourne
Scott D. Hughes

National Renewable Energy Laboratory
National Wind Technology Center
1617 Cole Boulevard
Golden, CO 80401, USA

Michael D. Zuteck
601 Clear Lake Road
MDZ Consulting
Kemah, TX 77565, USA

ABSTRACT

The ultimate strength of the PS Enterprises pultruded blade section was experimentally determined under four-point bending at the National Renewable Energy Laboratory. Thirteen 8-foot long full-scale blade segments were individually tested to determine their maximum moment carrying capability. Three airfoil-bending configurations were tested: high- and low-pressure skin buckling, and low pressure skin buckling with foam interior reinforcement. Maximum strain was recorded for each sample on the compressive and tensile surfaces of each test blade. Test data are compared to the results of three analytical buckling prediction methods. Based on deviations from the linear strain versus load curve, data indicate a post-buckling region. High-pressure side buckling occurred sooner than low-pressure side buckling. The buckling analyses were conservative for both configurations, but high-pressure side buckling in particular was substantially under-predicted. Both high- and low-pressure buckling configurations had very similar failure loads. These results suggests that a redundant load path may be providing strength to the section in the post-buckling region, making the onset of panel buckling a poor predictor of ultimate strength for the PS Enterprises pultrusion.

BACKGROUND

A turbine blade was developed by PS Enterprises (PSE) under a cost-shared subcontract with the National Renewable Energy Laboratory (NREL)[1]. The blade was developed for use on PSE's 85-kW wind turbine. This machine is a five-blade, downwind turbine equipped with an overspeed spoiler for RPM regulation. The primary objective of this development was to demonstrate lower fabrication costs through the use of a fiberglass composite pultrusion manufacturing process and low-solidity multi-bladed rotors.

The PSE rotor blades have a length of 7.56-m (297.5 in) and chord length of 0.346-m (13.6 in.). Blade construction used a vinyl ester/fiberglass pultrusion process to form the blade skin and spar structure. Pultrusion is an automated composite fabrication method in which bundles of dry fibers are mixed with resin as they are slowly drawn through a heated dye. The blade cures as it is pulled through the dye in a continuous "on-the-fly" process. The pultrusion process limits the blade to constant-chord and zero-twist

geometry with constant structural, aerodynamic, and material properties along its length. To provide a more optimum structure, the root is reinforced out to the 32% station using a secondary lay-up of exterior plys called "*doublers*", which provide additional structural stiffness and strength to the root. In addition, the interior cavities between the spars are filled with structural foam to provide panel stability to resist buckling. Static tests on this full blade structure were performed earlier at NREL's National Wind Technology Center (NWTC). Results from this test assessed the blade's load-carrying capability under an IEC class II hurricane load distribution, but an ultimate strength failure near the root attachment prevented a full understanding of the unmodified pultruded section [2].

The simplicity of the unmodified pultruded section geometry and the availability of multiple specimens, however, offered us an opportunity to take a more comprehensive look at the strength of just the pultruded section. This test program experimentally determined the strength of the pultruded section by testing multiple samples for three different configurations. We were able to take advantage of the constant spanwise properties and use a four-point bending test rig to simplify the loading. This paper describes this test program in which the buckling strength of the PSE airfoil section was determined, and investigates the effectiveness and potential advantages of the foam-filled versus non-foam-filled blades.

TEST ARTICLE DESCRIPTION

The 0.346-m (13.6-in.) airfoil shaped pultrusion under consideration has webs at 13%, 35%, and 60% of chord as shown in Figure 1. The skin on the high-pressure side of the blade has a nominal thickness of 2.72-mm (0.107-in.) Going inward from the outside surface, the layer by layer composition is 0.20-mm (.007-in.) Nexus veil, 0.25-mm (.010-in.) random mat, 0.38-mm (0.015-in.) +/- 45° double-bias stitched mat, 1.27-mm (0.050-in.) unidirectional roving, 0.38-mm (0.015-in.) +/- 45° double-bias stitched mat, and 0.25-mm (0.010-in.) random mat. The skin on the low-pressure (compression) side of the blade is thicker with a nominal thickness of 4.19-mm (0.165-in.). Going inward from the outside surface, the layer by layer composition is 0.20-mm (0.007-in.) Nexus veil, 0.25-mm (0.010-in.) random mat, 0.38-mm (0.015-in.) +/- 45° double-bias stitched mat, 2.74-mm (0.108-in.) unidirectional roving, 0.38-mm (0.015-in.) +/- 45° double-bias stitched mat, and 0.25-mm (0.010-in.) random mat.

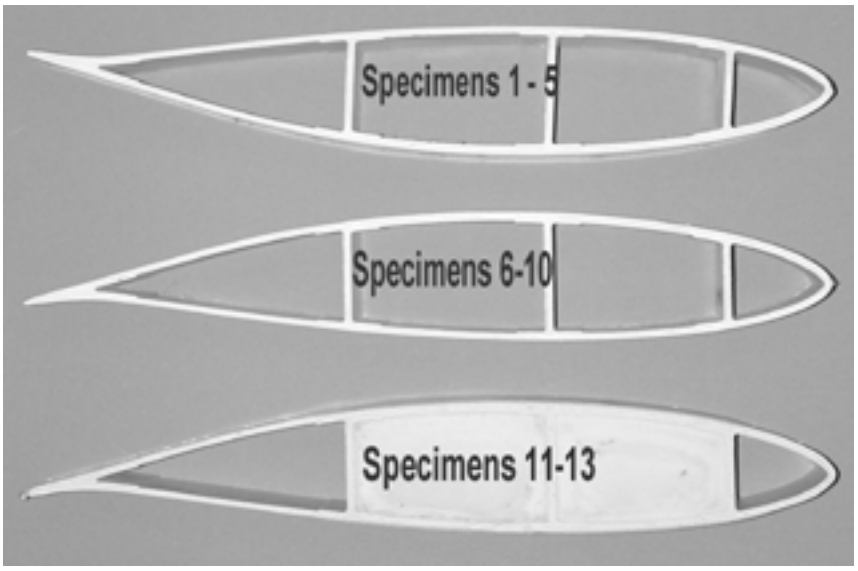

Figure 1 – Photo of PS Enterprises' Pultruded Cross Sections in Three Test Configurations

The Nexus veil of lightweight polyester fabric was used to provide a good exterior finish. Because it was thin and of low modulus, it was disregarded in the buckling analysis described later. This assumption provided some conservatism in the calculations, and left a symmetrical arrangement of layers to each side of the unidirectional "core" - to which the buckling calculations were best suited.

The panel most likely to initiate buckling was the one between the 35% and 60% webs, because for pure flatwise bending, it has slightly higher stress and longer unsupported span than the forward panel. Although the trailing edge panel has a longer span, its shell material is considerably closer to the flatwise-neutral bending plane, and would have lower stresses as a result. Analyses, therefore, were focused on the 35% - 60% panel.

A total of 13 samples were tested. PSE supplied 10 hollow specimens to NREL for the buckling tests; all cut by PSE to a length of 2.44-m (8-ft). Three additional 2.44-m (8-ft), foam-filled specimens were prepared at NREL from a full blade remaining from earlier tests. Figure 1 shows the cross-section of the PSE test samples in the three configurations tested. The upper section shown represents the section with the high-pressure surface in compression (blade specimens 1-5). This was predicted to be the weakest orientation and the orientation least likely to experience this loading because the wind loading under normal conditions keeps this surface in tension. The middle section represents the section with the low-pressure side in compression (blade specimens 6-10). This orientation is typical of true field conditions. The bottom section in Figure 1 shows the same low-pressure buckling orientation but with the foam-filled specimens (blade specimens 11-13).

EXPERIMENT DESCRIPTION

The tests were performed at the Industrial User Facility (IUF) high-bay testing area at the NWTC. All testing equipment was provided by NREL. The specimens were loaded using a four-point bending apparatus, shown in Figure 2. This apparatus allowed us to eliminate the root attachment

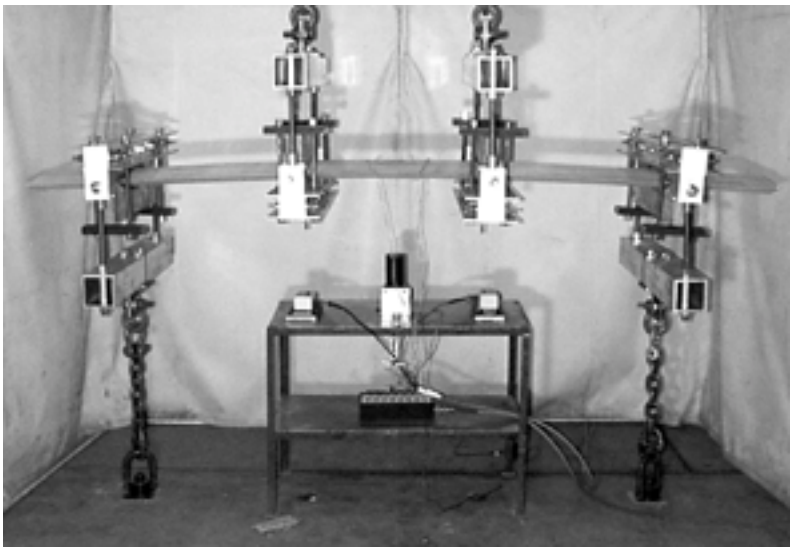

Figure 2 – Four-Point Bending Test Apparatus

hardware and drive the failures consistently into the constant-moment test section between the inner two saddles. The saddles were spaced 0.61-m (2-ft) apart along the specimen with 0.305-m (1-ft) extending out from each end. Each saddle was clamped around the blade, and gripped the blade with a 12.7-mm (0.50-in) thick layer of molded polyurethane. The two outer saddles were restrained by chains attached to imbedded inserts in the floor, 1.83-m (6-ft) apart. The two inner saddles were connected to an overhead spreader bar, consisting of a 0.91-m (3-ft) double C-channel strut. The testing load was applied to the center of this bar with a 311.4-kN (35-ton) capacity overhead bridge crane, to distribute the load-share evenly to the two inner saddles. A load cell was placed in the main load cable to measure the total force applied by the crane. Note that data shown in this paper are presented in terms of crane load. (To convert to the applied moment (kN-m) in the test section, the crane load (kN) should be multiplied by 0.61-m.)

A pivoting saddle design was used to minimize blade moments generated by the saddles themselves by introducing the loads at a pivot axis located at the airfoil section's chord-line.

INSTRUMENTATION AND DATA ACQUISITION

Blade surface strains, crane load, and deflections were measured during testing. Two strain gauges were centered at the middle of each test specimen, 1.21-m (4-ft) from the ends, on the high- and low-pressure sides at the 37% chord position. This position was chosen to be consistent with measurements made from previous tests and positioned to measure the maximum strain levels. A third gauge was added to 4 of the 13 test blades directly over the central spar at the 35%-pitch position, but this data is not presented. All gauges were single-element, 1000Ω (Measurements Group WK-09-250BF-10C) gauges and were oriented along the spanwise axis. Crane loads were measured using a HSI model 3100-70K, 311.4-kN (70,000-lb) load cell, positioned between the bridge crane and spreader bar.

Vertical displacements were measured using a single ultrasonic Senix Ultrasensor and 2 string pots. The Ultrasensor measured displacement of the center of the blade span, while one string pot measured the vertical displacement of each of the two inboard saddles. The combination of these three measurements with fixed outer saddles allowed an accurate representation of blade deflection along the length of the specimen. These data are given in Table 1.

A video camera was focused on the leading edge of the test specimen for all tests and positioned such that the entire testing apparatus (spreader bar, saddles, digital load display, and specimen) was visible at all stages of the test.

The NREL software program BSTRAIN, written in LabVIEW, was used as the front-end of the data acquisition system. Data was collected under static loading at a continuous sample rate of 10 Hz.

TEST PROCEDURE

For each specimen, the following setup procedure was followed. First, the two strain gauges were zeroed with the blade on the lab floor with zero moment applied, prior to mounting the specimen in the saddles. With the instrumentation still connected, the four load saddles were installed and attached to the crane and floor, respectively. The crane and load cell, with the test specimen attached, were raised until the weight of the specimen and load apparatus (tare load) were fully suspended by the crane, but with slack in the chains. Tare weight, which includes the weight of the spreader-bar, the test specimen, and the saddle assemblies, was 1278.7-N (288-lb) for the hollow specimens, and 1296-N (292-lb) for the foamed reinforced specimens. The displacement transducers and load cell were zeroed at the tare load, and two

cameras—one surface level and one ceiling-mounted—were started. The load was then increased in increments of 2220-N (500-lbf), until failure with a static dwell period of 20 seconds. All specimens were loaded to failure (See Figure 4). Figure 3 shows a sample loading history for these tests.

This procedure was repeated for all 13-blade specimens. The first five were oriented in the inverted position, the high-pressure panel placed in compression, and the second five were mounted in the saddles with the high-pressure panel in tension to simulate field conditions. The final three panels with foam-fill reinforcement were tested with the high-pressure panel in tension. After each test, the apparatus hardware was inspected for damage.

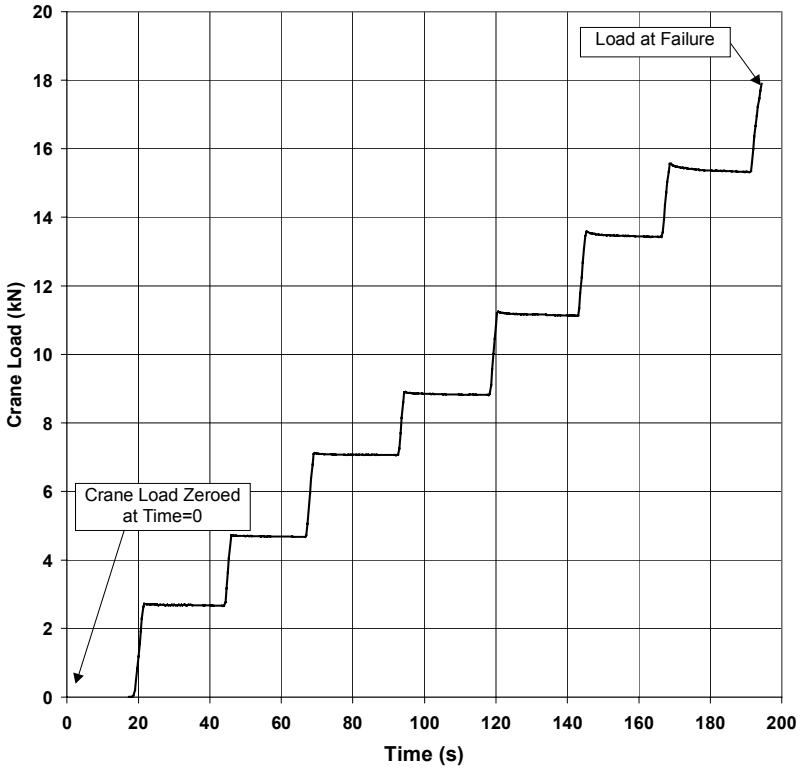

Figure 3. PSE Buckling Strength Test Time History

BUCKLING ANALYSIS

Before testing, buckling analyses were performed for the inverted and the non-inverted sections represented by blades 1-10. The layer thickness and longitudinal modulus values were supplied directly by the pultrusion manufacturer, and are briefly described in the section on test article description. The transverse and shear modulus values for the unidirectional roving were based on the data and volume fraction adjustment equation in the report DOE/MSU Composite Material Fatigue Database: Test Methods, Materials, and Analysis [3]. The remaining shear modulus values were estimates based on file data from other sources.

Three methods of analysis were used to predict buckling in the compressive panel between the 35% and 60% shear webs. The methods used were the Peery Method [4], the NACA TN 1928 Method [5], and the SCI Method [6]. The Peery Method is the simplest, and computes a panel stiffness contribution and a panel curvature contribution. The method comes from Dave Peery, author of the book *Aircraft*

Structures. The SCI method is based on work performed by Structural Composites Inc., which did considerable work on composite wind turbine blades for NASA, including buckling predictions of composite blades. All of these methods were for uniform shell materials, with only the SCI method including oriented material effects.

All analyses were performed using conservative assumptions regarding panel fixity. Panels were assumed to be pinned at the shear webs, with no resistance to panel rotation at the attachment points. No adjustments to the results of these analyses were made in this paper after learning the test results.

RESULTS

Figures 5 to 10 below provide tensile and compression-side strains for the blade samples of each orientation group. In Figures 5 and 6, the strains (high-pressure compressive) versus load for the inverted blades 1-5 shown at the top of Figure 1. Figures 7 and 8 show the strains (low-pressure compressive) versus load for the non-inverted blades 6-10 shown in the middle of Figure 1. Figures 9 and 10 show the strains (low-pressure compressive) versus load for the non-inverted, foam-reinforced blades 11- 13 shown at the bottom of Figure 1. Figure 11 shows failure loads for each specimen in a bar chart, and Table 1 lists results and relevant measurements. Along with the data, a straight line is shown in Figures 5-10 for reference so that linear deviations can be more easily distinguished.

Each of the compressive strain plots (Figures 5, 7, and 9) show that the blade skin panels experienced a period of linear behavior at low loads but eventually reached a point of instability where strain became uncorrelated with load. This point of instability is defined in this paper as the buckling limit, and is the point where we believe the blade skin panels between the 35% and the 60% shear webs began to experience out-of-plane deformations. In spite of this non-linear behavior, the blade samples continued to carry higher loads and eventually failed from 18% to 46% beyond the measured buckling limit.

Two vertical lines on each compressive plot mark the average buckling limit and the average failure load, respectively. The buckling limits were determined graphically from the strain versus load curves, and were selected as the point where instabilities were present on most blades as indicated by severe non-linear behavior. This method is subjective because it is dependent on consistent human interpretation but qualitatively it is useful to map the general data trends. The average failure strength is based on the average crane load at failure for the sample strengths plotted. The region between these two vertical lines is defined as the post-buckling zone. For each orientation, the size of this post-bucking zone appears to vary, which gives evidence that the onset of bucking is not well correlated with the sample strengths.

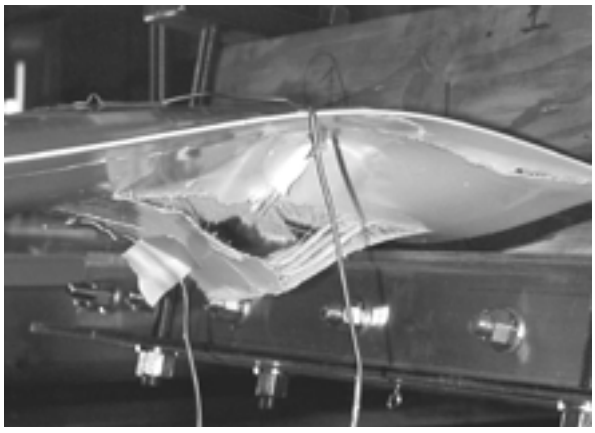

Figure 4 – Photo of Failed Section – High Pressure Side

For blades 1-5 (inverted), the buckling limit was the lowest with evidence of panel buckling appearing between 11-kN and 12-kN (2500-lbf and 2700-lbf). For blades 6-10 (non-inverted) buckling did not appear until 13-kN to 14-kN (2900-lbf to 3000-lbf). This trend is consistent with the buckling predictions shown in Figure 12, but the magnitudes of the analysis show that the actual buckling limits were higher than predicted. More surprising was that the average failure strength of 16.87 kN (3800-lbf) for blades 1–5 was nearly identical to the average strength of

blades 6-10. We expected that the lower buckling limit would have translated to lower failure strength but this did not occur. This result suggests that the buckling mode was not the primary cause of failure for these sections, and that an independent secondary mode was the primary cause of failure.

Each of the tensile stain plots (Figures 6, 8, and 10) show relatively linear behavior throughout the load history as was expected. A careful inspection of these plots, however, indicates that in the post-bucking zone, tensile strains become slightly non-linear and are probably picking up some additional strain due to the compression-side failure in progress.

Table 1 - Test Specimen Characteristics and Results

Blade	Resin System	Foam Core	Failure Load (kN)	Strain at Max Load: Compr/Tensile (ue)	Deflection Right Saddle (mm)	Deflection Center (mm)	Deflection Left Saddle (mm)	Stiffness (mm/kN)
1	Vinyl ester	No	17.95	4808 / 6947	94.16	106.05	95.07	5.27
2	Vinyl ester	No	18.49	6101 / 7421	104.42	115.93	104.27	5.64
3	Vinyl ester	No	15.14	8864 / 5671	83.69	95.28	81.66	5.46
4	Vinyl ester	No	16.33	2263 / 6161	85.34	98.37	85.32	5.23
5	Vinyl ester	No	16.49	4742 / 6483	87.05	95.73	89.48	5.35
6	Vinyl ester	No	16.60	6138 / 6181	77.60	NA	76.99	4.66
7	Vinyl ester	No	16.14	7079 / 6214	79.50	89.84	82.42	5.02
8	Vinyl ester	No	17.90	7668 / 6768	94.46	105.59	92.28	5.22
9	Vinyl ester	No	17.82	4878 / 7012	105.51	116.71	99.64	5.76
10	Vinyl ester	No	16.87	4563 / 6147	90.37	100.51	86.49	5.24
11	Polyester	Yes	20.11	6156 / 6314	94.44	106.07	93.73	4.68
12	Polyester	Yes	21.49	7762 / 6214	117.40	121.77	112.42	5.35
13	Polyester	Yes	19.03	NA/ 6215	88.09	98.50	87.63	4.62

The buckling limit of the foam-filled samples (blades 11 and 12) was approximately 17-kN to 18-kN (3800-lbf to 3900-lbf), which was the highest of any of the configurations tested (note that the strain gauge on blade 13 failed). The average failure strengths for these samples were also about 15% higher with average failure strength over 20 kN (4500-lbf). This result could indicate that the introduction of structural foam inside the section cavities can delay both the onset of buckling and section failure, but some cautions should be noted.

First, the exact structural properties of the foam were not know when this paper was written so these results cannot be used very broadly to estimate the generic ability of foam to delay buckling or strengthen composite airfoil sections.

Secondly, In Table 1, blade stiffness is calculated for each sample from the saddle deflection data. Stiffness was calculated as the average displacement of the right and left saddle divided by the crane load, and is expressed in units of mm/kN. From this data, the average stiffness of the foam-filled blades was about 10% greater than blades 1-10. The added stiffness is thought to be due to the foam. Blade 12, however, had approximately the same stiffness as the un-foamed blades, an anomaly that increases the uncertainty of the foam data. If blade 12 is ignored, the foam did not have a large affect on the strain at which buckling occurred for the other two samples. Therefore, it appears that the foam may simply increase the stiffness. Perhaps a better alternative might be to instead add this extra weight to the skin laminate where it could reduce buckling and add stiffness.

Finally, it should be noted that the foam-filled blades were manufactured using a polyester resin system, which is a variable that could influence the macroscopic properties of foam-filled samples. However, because of the poorer mechanical properties of polyester, we do not believe that its introduction into test samples for blades 11-13 would have significantly influenced the outcome of the strength tests [7]. Conversely, some data has shown that subtle improvements in compressive static strength can be realized in fiberglass/polyester coupons versus fiberglass/vinyl ester [3].

CONCLUSIONS

The ultimate strength of the PSE pultruded blade section was experimentally determined under four-point bending at NREL. Thirteen 2.44-m (8-ft) long full-scale blade segments were individually tested in three different configurations to determine their maximum moment carrying capability. Significant conclusions are as follows:

- The PSE pultruded sections have similar strength in positive and negative flatwise bending.
- Panel thickness, curvature, and laminate differences did not influence the failure strengths for the PSE section in the predicted manner.
- A post-buckling region existed for all blades and configurations before ultimate failure.
- The onset of panel buckling was not an accurate predictor of failure strength for the PSE sections.
- The simple buckling analysis models used to predict buckling for the PSE sections were not sufficient to determine when a section would fail.
- Buckling was not the principal failure mode determining ultimate strength for the PSE sections.
- Foam samples had higher ultimate strength in the PSE section but did little to change the strain at which buckling occurred. Multiple uncertainties gave us low confidence in the foam blade data.

ACKNOWLEDGMENTS

The authors would like to thank Kip Cheney of PS Enterprises for his cooperation and support in writing this paper. We would also like to thank Tim Olsen and Gene Quandt for helping with the test program over the years. We want to acknowledge the hard work of the other contributors of the structural testing team at NREL including Doug Cook, Darren DeShay, Randy Hunsberger, Mike Jenks, Manny Morrell, and Rick Santos. Finally, we would like to thank the U.S. Department of Energy for their continued support of structural testing at NREL.

REFERENCES

1. Cheney, M.C.; Olsen, T.; Quandt, G.; Arcidiacono, P. *Analysis and Tests of Pultruded Blades for Wind Turbine Rotors*, NREL/SR-500-25949, July 1999.
2. Musial, W.D. ; Hughes, S.; Johnson, J.; Jenks, M.; Deshay, D.; Egging, N. *PS Enterprises – 85 kW Blade Full Scale Static Testing*. NREL internal report. 23 April 1997.
3. Mandell J.F.; Samborsky, D.D. *DOE/MSU Composite Material Fatigue Database: Test Methods, Materials, and Analysis*, SAND97-3002, Sandia National Laboratories, Albuquerque, NM.
4. Peery, D. *Aircraft Structures*, McGraw Hill, 1950.
5. Bruhn, E.F.; Bollard, R.J.H; et al. *Analysis And Design of Flight Vehicle Structures,* Indianapolis: S.R.Jacobs, c1973
6. Wiengart, O. *Design, Evaluation, and Fabrication of Low-Cost Composite Blades for Intermediate-Sized Wind Turbines*, Structural Composites Industries, Inc., September 1981.
7. *Engineered Materials Handbook, Volume 1, Composites*, ASM International, 1987.

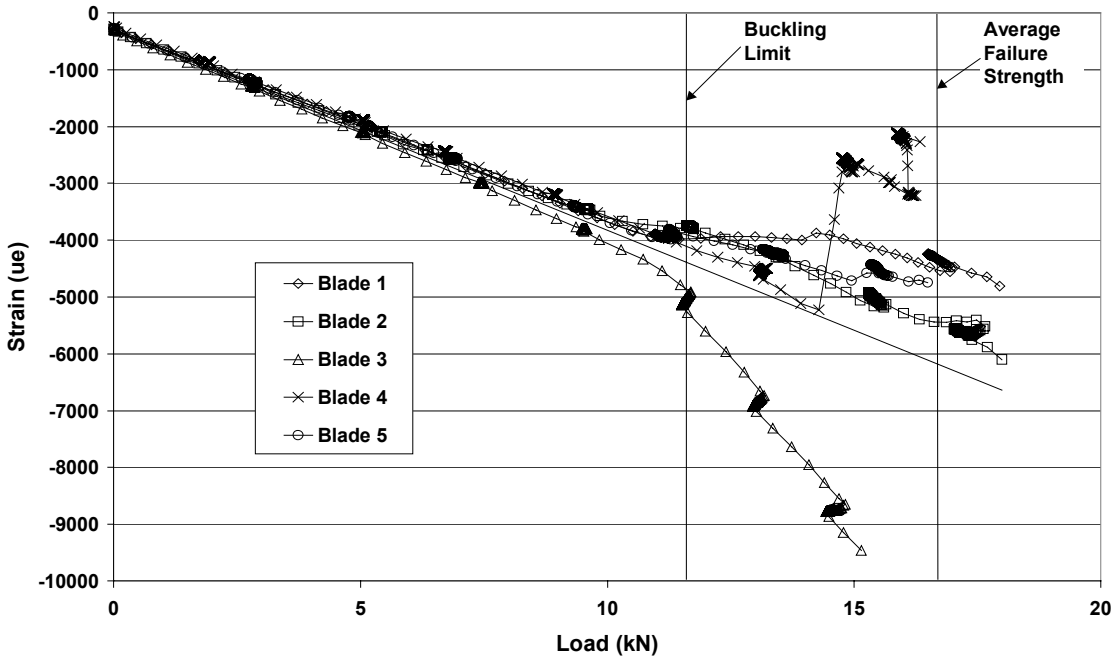

Figure 5 – Compressive Strains for Specimens 1-5

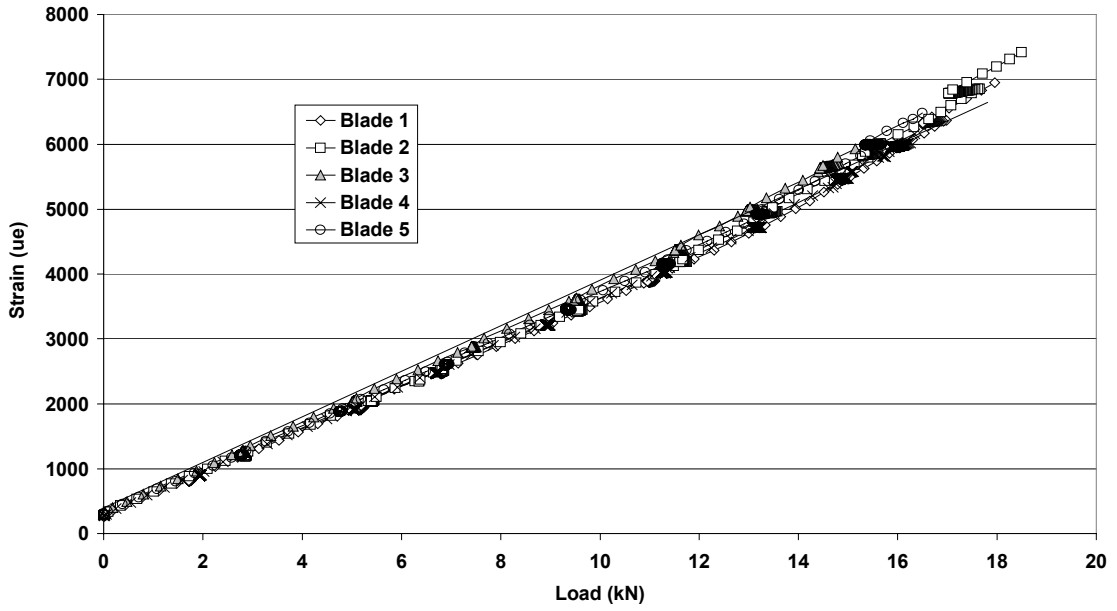

Figure 6 – Tensile Strains for Specimens 1-5

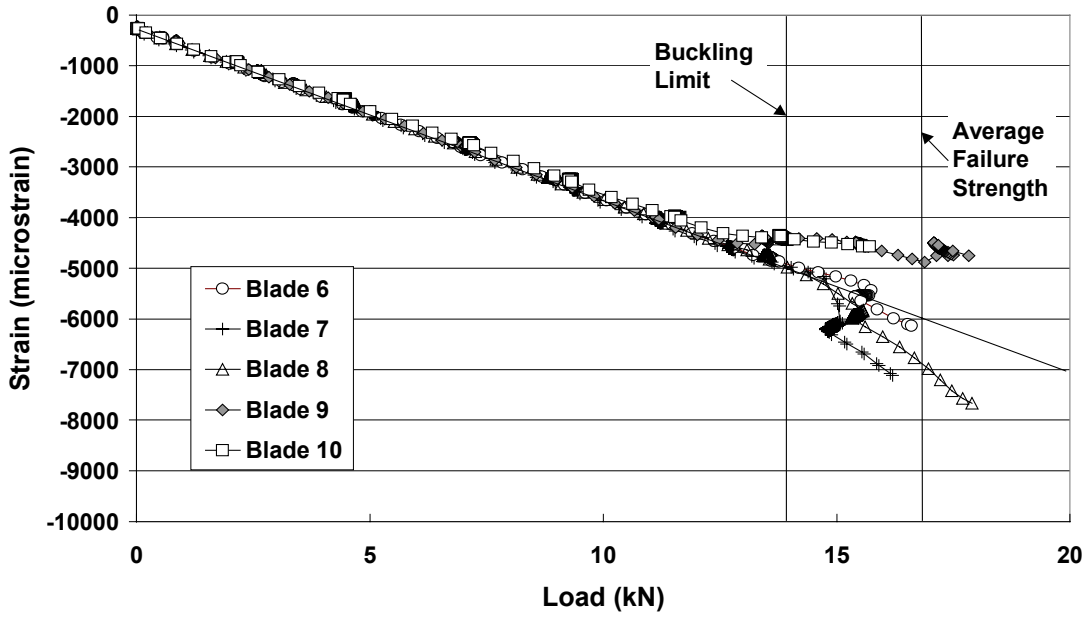

Figure 7 – Compressive Strains for Specimens 6-10

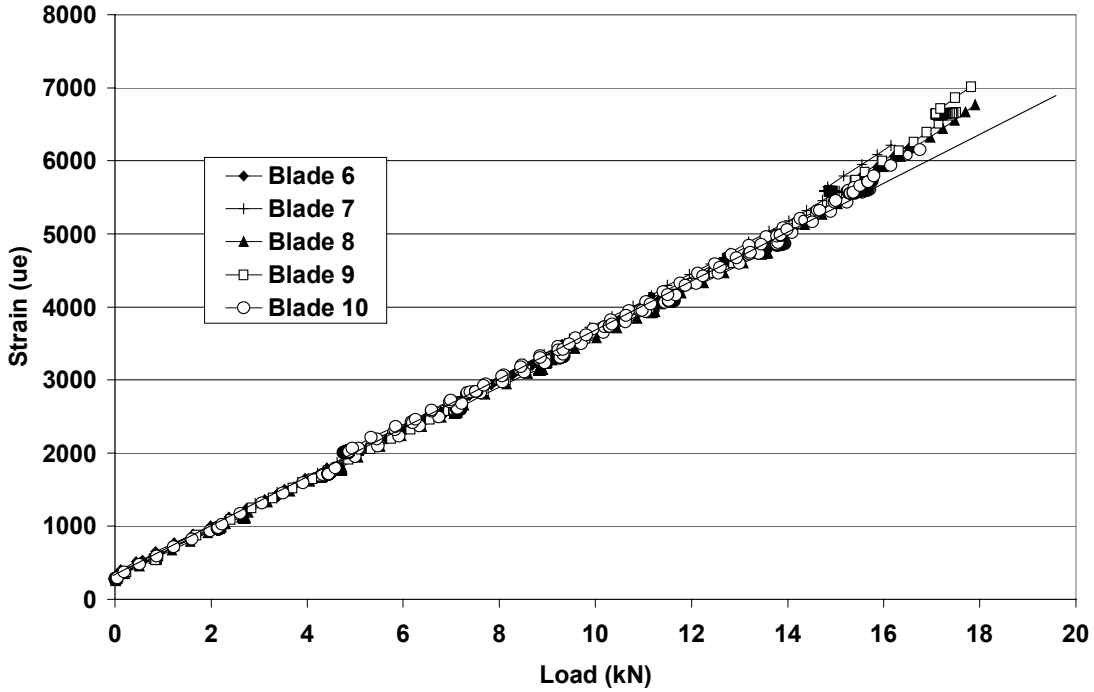

Figure 8 – Tensile Strains for Specimens 6-10

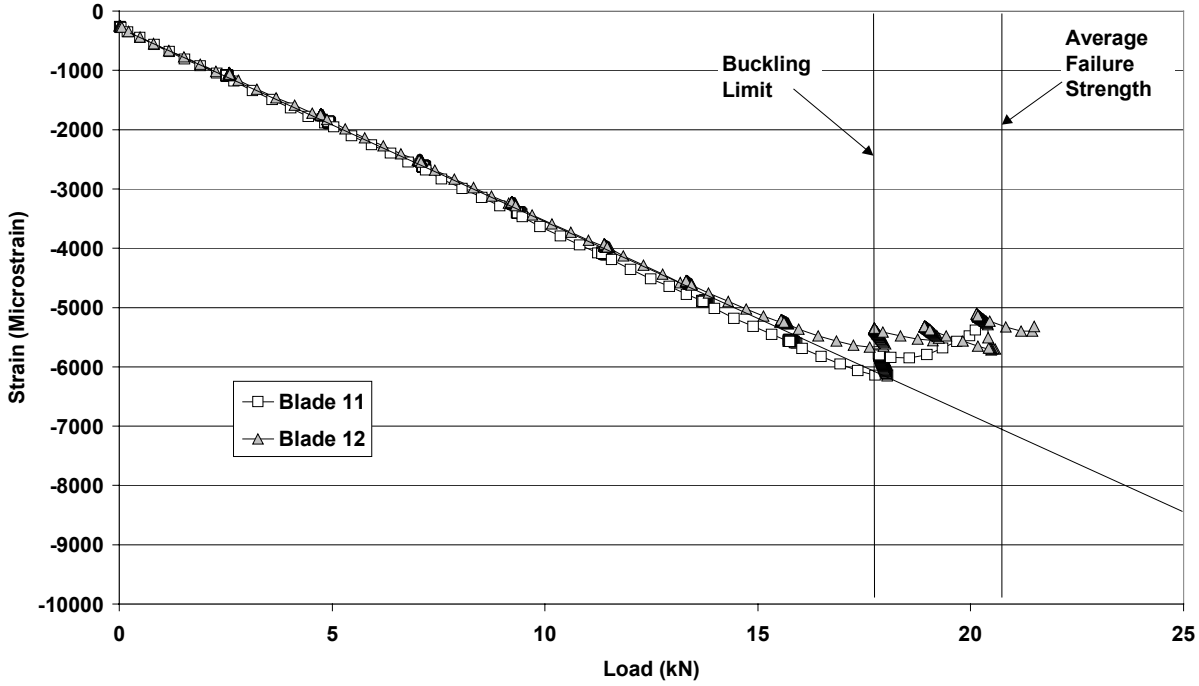

Figure 9 – Compressive Strains for Specimens 11-13

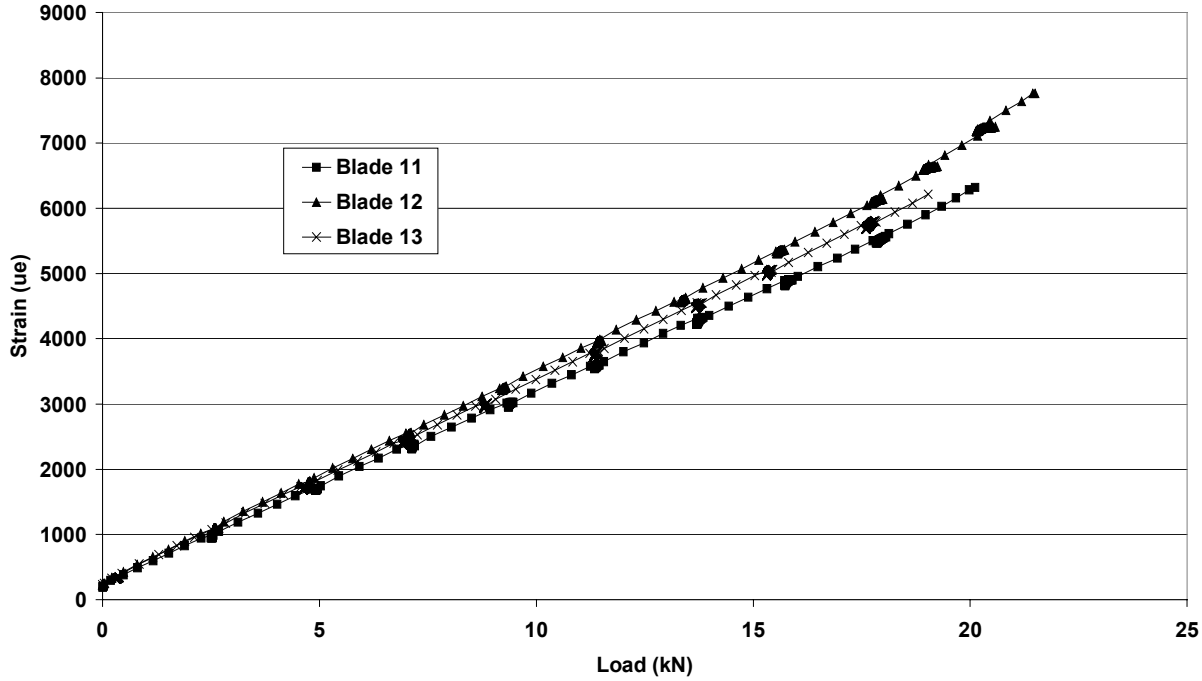

Figure 10 – Tensile Strains for Specimens 11-13

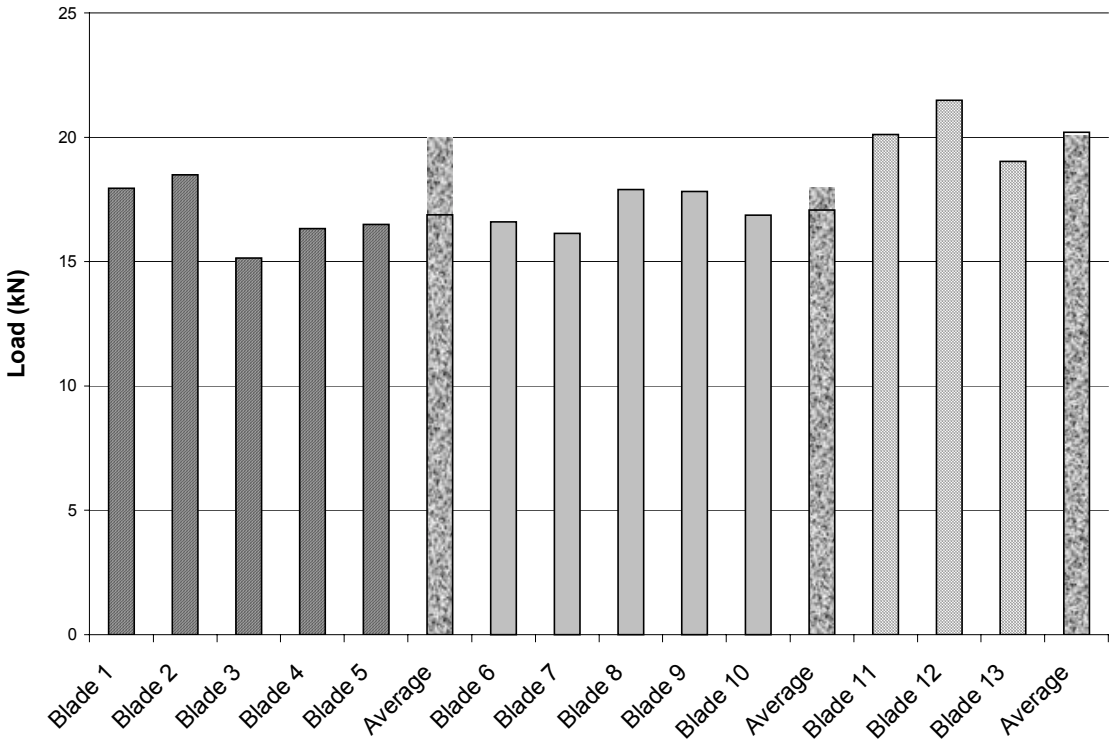

Figure 11 – Failure Strength Summary for All Specimens

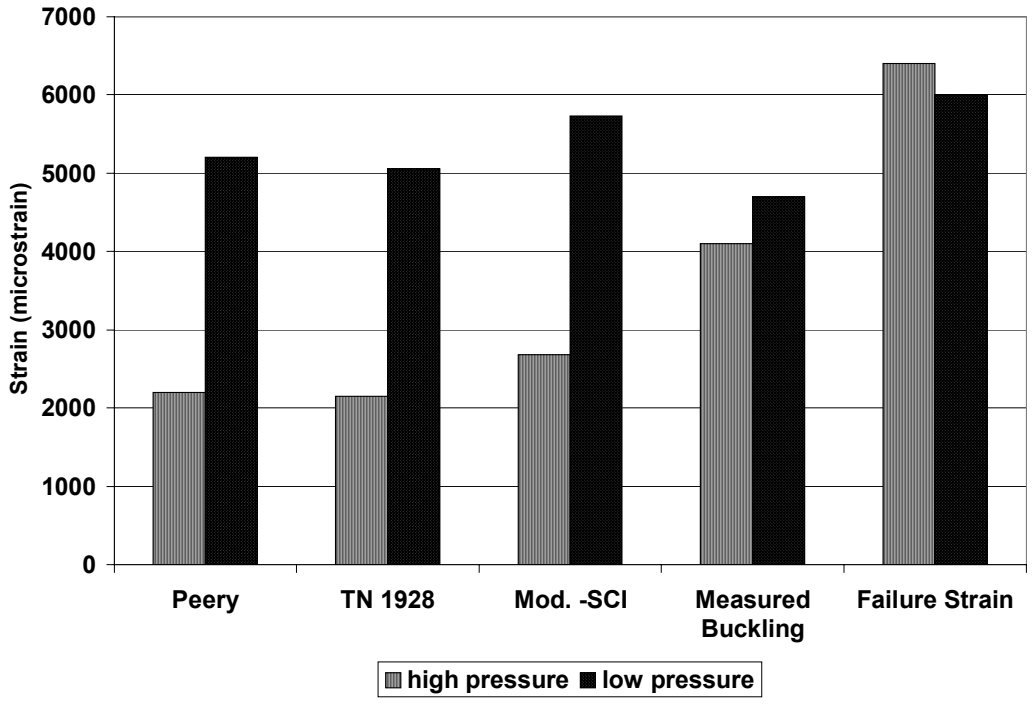

Figure 12 – Comparison of Buckling and Failure Strengths with Predictions

REPORT DOCUMENTATION PAGE

Form Approved
OMB NO. 0704-0188

1. AGENCY USE ONLY (Leave blank)	2. REPORT DATE	3. REPORT TYPE AND DATES COVERED
	September 2001	Conference paper

4. TITLE AND SUBTITLE
Four-Point Bending Strength Testing of Pultruded Fiberglass Composite Wind Turbine Blade Sections

5. FUNDING NUMBERS
WER1.2450

6. AUTHOR(S)
Walter D. Musial, Ben Bourne, Scott D. Hughes, Michael D. Zuteck

7. PERFORMING ORGANIZATION NAME(S) AND ADDRESS(ES)

8. PERFORMING ORGANIZATION REPORT NUMBER

9. SPONSORING/MONITORING AGENCY NAME(S) AND ADDRESS(ES)
National Renewable Energy Laboratory
1617 Cole Blvd.
Golden, CO 80401-3393

10. SPONSORING/MONITORING AGENCY REPORT NUMBER
NREL/CP-500-30565

11. SUPPLEMENTARY NOTES
NREL Technical Monitor: NA

12a. DISTRIBUTION/AVAILABILITY STATEMENT
National Technical Information Service
U.S. Department of Commerce
5285 Port Royal Road
Springfield, VA 22161

12b. DISTRIBUTION CODE

13. ABSTRACT *(Maximum 200 words)*

The ultimate strength of the PS Enterprises pultruded blade section was experimentally determined under four-point bending at the National Renewable Energy Laboratory. Thirteen 8-foot long full-scale blade segments were individually tested to determine their maximum moment carrying capability. Three airfoil-bending configurations were tested: high- and low-pressure skin buckling, and low pressure skin buckling with foam interior reinforcement. Maximum strain was recorded for each sample on the compressive and tensile surfaces of each test blade. Test data are compared to the results of three analytical buckling prediction methods. Based on deviations from the linear strain versus load curve, data indicate a post-buckling region. High-pressure side buckling occurred sooner than low-pressure side buckling. The buckling analyses were conservative for both configurations, but high-pressure side buckling in particular was substantially under-predicted. Both high- and low-pressure buckling configurations had very similar failure loads. These results suggests that a redundant load path may be providing strength to the section in the post-buckling region, making the onset of panel buckling a poor predictor of ultimate strength for the PS Enterprises pultrusion.

14. SUBJECT TERMS
wind energy; wind turbine blade testing; airfoils

15. NUMBER OF PAGES

16. PRICE CODE

17. SECURITY CLASSIFICATION OF REPORT	18. SECURITY CLASSIFICATION OF THIS PAGE	19. SECURITY CLASSIFICATION OF ABSTRACT	20. LIMITATION OF ABSTRACT
Unclassified	Unclassified	Unclassified	UL